

Shape/Size-Controlled Syntheses of Metal Nanoparticles for Site-Selective Modification of Carbon Nanotubes

Liangti Qu,[†] Liming Dai,^{*,†,‡} and Eiji Osawa[§]

Contribution from the Department of Chemical and Materials Engineering, School of Engineering, University of Dayton, 300 College Park, Dayton, Ohio 45469-0240, University of Dayton Research Institute, Dayton 45469, and NanoCarbon Research Institute, Ltd., c/o Toudai Kashiwa Venture Plaza, 5-4-19 Kashiwa-no-ha, Kashiwa, Chiba 277-0882, Japan

Received January 15, 2006; E-mail: ldai@udayton.edu

Abstract: Shape- and size-controlled syntheses of metal nanoparticles have been achieved by galvanic displacement reaction between an aqueous solution of metal salt and Cu foil substrate. In particular, cubic and spheric nanoparticles of Pt (Au) with a fairly narrow size distribution were produced by reacting K_2PtCl_4 ($HAuCl_4$) with a Cu foil in an aqueous medium with and without $CuCl_2$ under different reaction conditions (e.g., different concentrations and reaction times). In conjunction with the substrate-enhanced electrodeless deposition (SEED) technique (Qu, L.; Dai, L. *J. Am. Chem. Soc.* **2005**, *127*, 10806), the shape/size-controlled syntheses have been successfully exploited to *site-selectively* deposit these metal nanoparticles onto the outerwall, innerwall, or end-tip of carbon nanotubes (CNTs). Asymmetric sidewall modification by attaching the innerwall and outerwall of CNTs with metal nanoparticles of different shapes was also achieved. Furthermore, it was demonstrated that the nanotube-supported Pt nanoparticles could be converted into hollow Au nanoboxes by galvanic displacement of Pt with Au. These CNT-supported metal nanoparticles were shown to possess interesting optical and electrocatalytic properties.

Introduction

With the recent development in nanomaterials and nanotechnology,^{1–3} research on nanoparticles, in general, and metal nanoparticles, in particular, has received renewed interest in recent years for their potential applications in photography, catalysis, biological labeling, photonics, optoelectronics, information storage, surface-enhanced Raman scattering (SERS), and many other areas.^{4–7} Like many other nanomaterials, metal nanoparticles show shape/size-dependent properties.⁸ Conse-

quently, much effort has been devoted to the shape and size-controlled syntheses of metal nanoparticles.⁹

On the other hand, multicomponent assemblies of nanoscale entities are attractive for multifunctional systems, including optoelectronic,¹⁰ sensing, and catalysis.¹¹ In this context, a few innovative methods have been devised to graft metal nanoparticles onto carbon nanotube (CNT) structures.¹² These metal nanoparticles may act as quantum dot devices along the nanotube molecular wires of one-dimensional electronic properties, and they may also serve as active sites for further modification and assembling of CNTs. The detailed structure and precise location of the metal nanoparticles along the nanotube molecular wires plays an important role in regulating the final assembled structure and its performance. As far as we

[†] University of Dayton.

[‡] University of Dayton Research Institute.

[§] NanoCarbon Research Institute.

- (1) Meyyappan, M. *Carbon Nanotubes: Science and Applications*; CRC Press: Boca Raton, FL, 2005.
- (2) Dai, L. *Intelligent Macromolecules for Smart Devices: From Materials Synthesis to Device Applications*; Springer-Verlag: New York, 2004.
- (3) Baughman, R. H.; Zakhidov, A. A.; de Heer, W. A. *Science* **2002**, *297*, 787 and references therein.
- (4) (a) Lam, D. M.-K.; Rossiter, B. W. *Sci. Am.* **1991**, *265*, 80. (b) Tani, T. *J. Dispersion Sci. Technol.* **2004**, *25*, 375. (c) Lewis, L. N. *Chem. Rev.* **1993**, *93*, 2693.
- (5) Nicewarner-Pena, S. R.; Freeman, R. G.; Reiss, B. D.; He, L.; Pena, D. J.; Walton, I. D.; Cromer, R.; Keating, C. D.; Natan, M. J. *Science* **2001**, *294*, 137.
- (6) (a) Maier, S. A.; Brongersma, M. L.; Kik, P. G.; Meltzer, S.; Requicha, A. A. G.; Atwater, H. A. *Adv. Mater.* **2001**, *13*, 1501. (b) Krenn, J. R. *Nat. Mater.* **2003**, *2*, 210. (c) Kamat, P. V. *J. Phys. Chem. B* **2002**, *106*, 7729. (d) Seker, F.; Malenfant, P. R. L.; Larsen, M.; Alizadeh, A.; Conway, K.; Kulkarni, A. M.; Goddard, G.; Garaas, R. *Adv. Mater.* **2005**, *17*, 1941. (e) Murray, C. B.; Sun, S.; Doyle, H.; Betley, T. *Mater. Res. Soc. Bull.* **2001**, *26*, 985.
- (7) (a) Nie, S.; Emory, S. R. *Science* **1997**, *275*, 1102. (b) Dick, L. A.; McFarland, A. D.; Haynes, C. L.; Van Duyne, R. P. *J. Phys. Chem. B* **2002**, *106*, 853.
- (8) See, for example: (a) Sun, Y. G.; Xia, Y. N. *Analyst* **2003**, *128*, 686. (b) Jana, N. R.; Gearheart, L.; Obare, S. O.; Murphy, C. J. *Langmuir* **2002**, *18*, 922. (c) Salzmann, C.; Lisiecki, I.; Brioude, A.; Urban, J.; Pileni, M. P. *J. Phys. Chem. B* **2004**, *108*, 13242.

- (9) See, for example: (a) Sun, Y. G.; Xia, Y. N. *Science* **2002**, *298*, 2176. (b) Puentes, V. F.; Krishnan, K. M.; Alivisatos, A. P. *Science* **2001**, *291*, 2115. (c) Ahmadi, T. S.; Wang, Z. L.; Green, T. C.; Henglein, A.; El-Sayed, M. A. *Science* **1996**, *272*, 1924. (d) Wang, Z. L.; Mohamed, M. B.; Link, S.; El-Sayed, M. A. *Surf. Sci.* **1999**, *440*, L809. (e) Kim, F.; Connor, S.; Song, H.; Kuykendall, T.; Yang, P. D. *Angew. Chem. Int. Ed.* **2004**, *43*, 3673. (f) Shankar, S. S.; Rai, A.; Ankanwar, B.; Singh, A.; Ahmad, A.; Sastry, M. *Nat. Mater.* **2004**, *3*, 482.
- (10) (a) Kovtyukhova, N. I.; Kelley, B. K.; Mallouk, T. E. *J. Am. Chem. Soc.* **2004**, *126*, 12738. (b) Wu, Y.; Fan, R.; Yang, P. *Nano Lett.* **2002**, *2*, 83. (c) Gudiksen, M. S.; Lauthon, L. J.; Wang, J.; Smith, D. C.; Lieber, C. M. *Nature* **2002**, *415*, 617.
- (11) (a) Davis, J. J.; Coleman, K. S.; Azamian, B. R.; Bagshaw, C. B.; Green, M. L. H. *Chem. Eur. J.* **2003**, *9*, 3732. (b) Maillard, F.; Lu, G. Q.; Wieckowski, A.; Stimming, U. *J. Phys. Chem. B* **2005**, *109*, 16230.
- (12) (a) Choi, H. C.; Shim, M.; Bangsaruntip, S.; Dai, H. *J. Am. Chem. Soc.* **2002**, *124*, 9058. (b) Li, J.; Moskovits, M.; Haslett, T. L. *Chem. Mater.* **1998**, *10*, 1963. (c) Moghaddam, M. J.; Taylor, S.; Gao, M.; Huang, S.; Dai, L.; McCall, M. J. *Nano Lett.* **2004**, *4*, 89. (d) Quinn, B.; Dekker, C.; Lemay, S. J. *Am. Chem. Soc.* **2005**, *127*, 6146. (e) Mieszawska, A. J.; Jalilian, R.; Sumanasekera, G. U.; Zamborini, F. P. *J. Am. Chem. Soc.* **2005**, *127*, 10822.

are aware, however, almost no attention has been paid to the shape/size-controlled syntheses of metal nanoparticles for site-selective modification of CNTs by attaching the nanotube innerwall, outerwall, and/or end-tip(s) with metal nanoparticles of different shapes in a controllable fashion.

In the present study, we found that the shape- and size-controlled syntheses of metal nanoparticles (e.g., Pt, Au) could be achieved by simply reacting appropriate aqueous solutions (e.g., K_2PtCl_4 , $HAuCl_4$) with a Cu foil via a galvanic displacement reaction at different metal ion concentrations and/or reaction times. Galvanic displacement reactions, involving concurrent electrochemical oxidation and reduction, have been widely used to deposit metal nanoparticles on metallic or semiconducting substrates.¹³ The driving force for the galvanic displacement reaction arises from the difference in half-cell potentials between the metal ions to be reduced and the substrate to be oxidized. For the deposition of metal nanoparticles, the half-cell potential of the reduced species must be higher than that of the oxidized substrate. Accordingly, we found that Pt or Au nanospheres and nanocubes with a narrow size distribution can be directly deposited onto a Cu foil without any additional reducing or capping reagents (e.g., polyvinylpyridine, PVP, and silver ions^{9a,e,13a}). This, together with our previously reported substrate-enhanced electroless deposition (SEED) technique,¹⁴ prompted us to deposit metal nanoparticles of a controllable shape and size onto CNTs in a site-selective manner. In this paper, we report the first site-selective modification of the outerwall, innerwall, or end-tip(s) of either aligned or nonaligned CNTs with the shape/size-controlled metal nanoparticles. Asymmetric sidewall modification with the outerwall and innerwall of individual CNTs being attached by metal nanoparticles of different shapes will also be described.

Experimental Section

Materials. Potassium tetrachloroplatinate(II) (K_2PtCl_4) and hydrogen tetrachloroaurate (III) ($HAuCl_4$) were purchased from Aldrich and Alfa Aesar, respectively, and were used as received. Copper foils were obtained from EMS US. CNTs for the outerwall and tip modification were prepared by pyrolysis of iron (II) phthalocyanine (FePc),¹⁵ while those for the innerwall and asymmetric sidewall modification were produced by the template-synthesis method using commercially available alumina membrane (Whatman) templates with pore size of about 200–500 nm according to the reported procedure.¹⁶

Controlled Syntheses of Metal Nanoparticles. In a typical experiment, Pt (Au) nanoparticles were produced by immersing Cu foils into an aqueous solution of K_2PtCl_4 ($HAuCl_4$) at room temperature for a certain period of time, followed by thoroughly rinsing with distilled water. We used a low metal salt concentration (≤ 1.9 mM) for the formation of spheric nanoparticles. However, a relatively high metal salt concentration (≥ 3.8 mM), with or without the addition of $CuCl_2$, was used for the nanocube formation (vide infra). Au nanoparticles

with spherical and cubic structures can also be synthesized with aqueous solutions of $HAuCl_4$ under similar experimental conditions.

Outerwall Modification of CNTs with Pt Nanocubes and Nanospheres. To attach Pt nanocubes onto the nanotube outerwall, we deposited 10 droplets (~ 0.5 mL) of MWNTs dispersed in ethanol (0.8 mg/10 mL) onto a Cu foil (8 cm²). Having been dried in air, the Cu-supported CNTs were immersed into an aqueous solution of 3.8 mM K_2PtCl_4 containing 5 mM $CuCl_2$ for 1 min and then thoroughly washed with distilled water. Following the same procedure, the Cu foil-supported CNTs were reacted with 0.95 mM K_2PtCl_4 in the absence of $CuCl_2$ for 30 min to deposit Pt nanospheres onto the nanotube outerwall.

Conversion of the CNT-Supported Pt Nanocubes into Au Nanoboxes. The above-mentioned Pt nanocube-modified CNTs supported by the Cu foil were ultrasonicated (VWR model 75D ultrasonication bath) and dispersed in distilled water (1.6 mL). To eight droplets of this aqueous solution of the Pt nanocube-modified CNTs was added one droplet of 1 mM $HAuCl_4$ aqueous solution. The reaction mixture was then kept at room temperature for 20 min, leading to the formation of Au hollow nanoboxes along the CNT structure. The resultant Au nanobox-modified CNTs were collected by centrifuging and repeatedly washed with distilled water.

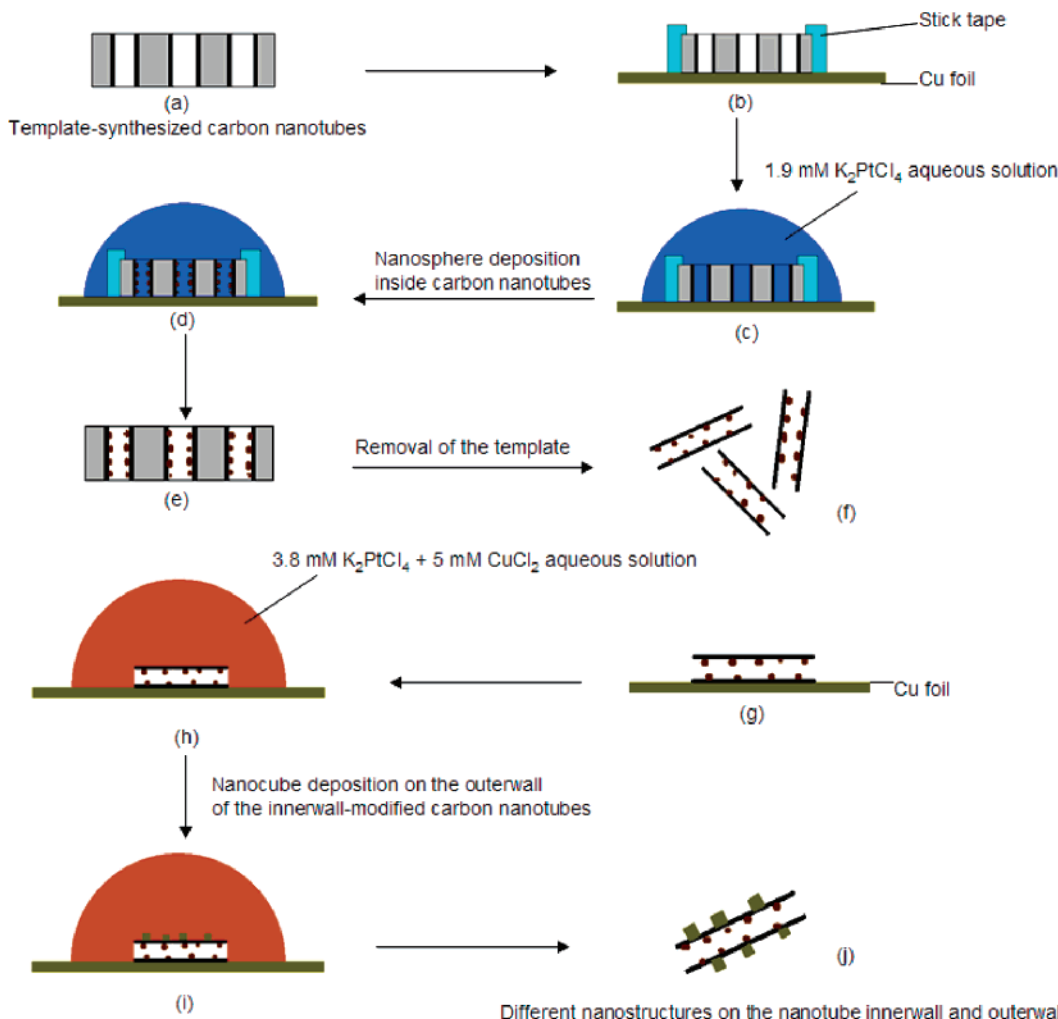
Modification of Aligned CNTs with Pt Nanocubes. An aligned CNT film generated by pyrolysis of FePc was removed from the quartz plate as a free-standing film in an aqueous HF solution (ca. 10 wt %/wt),^{15b} followed by carefully washing with distilled water. The free-standing nanotube film was then held on a Cu foil by stick tapes at the film edge. The nanotube film was kept undried during the whole course of the sample preparation so that both the top surface of the CNT film and the nanotube outerwall were accessible by an aqueous solution of metal salt. An alternative option to maximize the access for the metal salt aqueous solution was to render the nanotube sidewall hydrophilic by keeping the aligned CNT film in H_2SO_4/HNO_3 for several hours before the surface modification. Pt nanocubes were then deposited along the aligned CNT length by immersing the above prewetted/preactivated aligned CNT film supported by the Cu foil into an aqueous solution of 3.8 mM K_2PtCl_4 containing 5 mM $CuCl_2$ for 1 min.

Modification of the Nanotube Innerwall and Asymmetric Sidewall Modification with Metal Nanospheres and Nanocubes. Scheme 1 shows the procedures for modification of the nanotube innerwall and the asymmetric sidewall modification with Pt nanospheres being attached on the nanotube innerwall and nanocubes on the outerwall. To facilitate the introduction of the metal salt solution into the nanotube hollow core, we first immersed the template-synthesized aligned CNTs within the alumina membrane (Scheme 1a) into an aqueous solution of 1.9 mM K_2PtCl_4 under ultrasonication for 5 min. After removing the remaining solution on the surface of alumina membrane by adsorption with a filter paper, the preactivated alumina membrane-supported aligned CNT film was *perpendicularly* anchored onto a copper foil by stick tapes (Scheme 1b) and then reimmersed into the aqueous solution of 1.9 mM K_2PtCl_4 for 30 min for the formation of Pt nanospheres on the nanotube innerwall (Scheme 1, parts c and d). Subsequently, the innerwall-modified CNTs (Scheme 1e) were released from the alumina membrane using an aqueous HF solution (Scheme 1f). To demonstrate the asymmetric sidewall modification, we deposited the innerwall-modified nanotubes onto a Cu foil with a *sidewall-on* configuration (Scheme 1g) before being exposed to an aqueous solution of 3.8 mM K_2PtCl_4 containing 5 mM $CuCl_2$ for 1 min. The resultant asymmetrically modified CNTs (Scheme 1h–j) were then thoroughly washed with distilled water and characterized on a scanning electron microscopy (SEM) and transmission electron microscopy (TEM).

Tip Modification of CNTs with Pt Nanocubes and Nanospheres. To demonstrate the tip modification, we used the perpendicularly aligned CNTs produced by pyrolysis of FePc.¹⁵ In particular, we removed the FePc-generated aligned CNT film from the quartz substrate as a free-standing film in an aqueous HF solution (ca. 10 wt %/wt),^{15b}

- (13) See, for example: (a) Song, H.; Kim, F.; Connor, S.; Somorjai, G. A.; Yang, P. D. *J. Phys. Chem. B* **2005**, *109*, 188. (b) Dryfe, R. A. W.; Walter, E. C.; Penner, R. M. *ChemPhysChem* **2004**, *5*, 1879. (c) Magagnin, L.; Maboudian, R.; Carraro, C. *J. Phys. Chem. B* **2002**, *106*, 401. (d) Porter, L. A.; Choi, H. C.; Schmeltzer, J. M.; Ribbe, A. E.; Elliott, L. C. C.; Buriak, J. M. *Nano Lett.* **2002**, *2*, 1369. (e) Aizawa, M.; Cooper, A. M.; Malac, M.; Buriak, J. M. *Nano Lett.* **2005**, *5*, 815.
- (14) Qu, L. T.; Dai, L. *J. Am. Chem. Soc.* **2005**, *127*, 10806.
- (15) (a) Li, D. C.; Dai, L.; Huang, S.; Mau, A. W. H.; Wang, Z. L. *Chem. Phys. Lett.* **2000**, *316*, 349. (b) Huang, S.; Dai, L.; Mau, A. W. H. *J. Phys. Chem. B* **1999**, *103*, 4223.
- (16) (a) Che, G.; Lakshmi, B. B.; Martin, C. R.; Fisher, E. R.; Ruoff, R. S. *Chem. Mater.* **1998**, *10*, 260. (b) Miller, S. A.; Young, V. Y.; Martin, C. R. *J. Am. Chem. Soc.* **2001**, *123*, 12335.

Scheme 1. Procedures for the Nanotube Innerwall Modification and the Asymmetric Modification of the Nanotube Innerwall with Pt Nanospheres and the Outerwall with Nanocubes^a



^aFor the sake of clarity, only a few of the many CNTs on the Cu foil are shown.

which was then perpendicularly anchored onto a Cu foil by stick tapes (Scheme 1b). Having been thoroughly washed with distilled water, the Cu foil-supported aligned CNT film was then floated on aqueous K_2PtCl_4 solutions of different concentrations with each of the constituent CNTs within the aligned nanotube film perpendicularly aligned at the air/liquid interface¹⁷ for depositing Pt nanoparticles on the nanotube end-tips only. An aqueous solution of 3.8 mM K_2PtCl_4 containing 5 mM $CuCl_2$ and a deposition time of 1 min were used for the deposition of Pt nanocubes, while Pt nanospheres were deposited onto the nanotube tips from an aqueous solution of 0.95 mM K_2PtCl_4 with a deposition time of 30 min.

Characterization and Optoelectronic Properties. SEM imaging was performed on a Hitachi S-4800 high-resolution scanning electron microscope. An energy-dispersive X-ray spectroscopic (EDS) detecting unit was used for the element analysis. TEM images and electron diffraction (ED) patterns were taken on a Hitachi H-7600 transmission electron microscope. UV–vis spectra were recorded on a Lambda 900 UV/VIS/NIR spectrometer (Perkin-Elmer).

Electrochemical measurements were carried out in a single-compartment, three-electrode glass cell with a KCl-saturated Ag/AgCl reference electrode and a platinum counter electrode. A Pt nanocube-grafted aligned CNT film of 4 mm² supported by a thin layer of sputter-coated Au was used as the working electrode, while a similar pristine aligned CNT film was also measured for comparison. N_2 -saturated solution

containing 2 M CH_3OH + 0.1 M H_2SO_4 was used as the electrolyte. Cyclic voltammetric measurements were performed with a scan rate of 50 mV s⁻¹ on an eDAQ potentiostat electrochemical analyzer (Australia).

Results and Discussion

1. Shape/Size-Controlled Synthesis of Metal Nanoparticles.

1.1. Shape-Controlled Syntheses of Metal Nanoparticles.

Figure 1 shows SEM images of Pt nanostructures obtained by a typical galvanic displacement reaction^{13,18} between Cu foils and aqueous K_2PtCl_4 solutions of different concentrations for a constant deposition time of 30 min. Interestingly, both spherical and cubic nanostructures were produced, and a concentration-dependent shape evolution was clearly evident. Figure 1, parts a and b, shows the formation of smooth Pt nanoparticles between 150 and 400 nm in diameter when Cu foil was immersed into aqueous solutions of K_2PtCl_4 at low concentrations (≤ 1.9 mM). Upon increasing the metal salt concentration up to about 3.8 mM, Pt cubic nanoparticles of a fairly uniform size (150–300 nm in the side length) were formed (Figure 1c). Further increasing the metal salt concentration caused the nanocubes

(17) Lee, K.; Li, L.; Dai, L. *J. Am. Chem. Soc.* **2005**, *127*, 4122.

(18) (a) Porter, L. A.; Choi, H. C.; Ribbe, A. E.; Buriak, J. M. *Nano Lett.* **2002**, *2*, 1067.

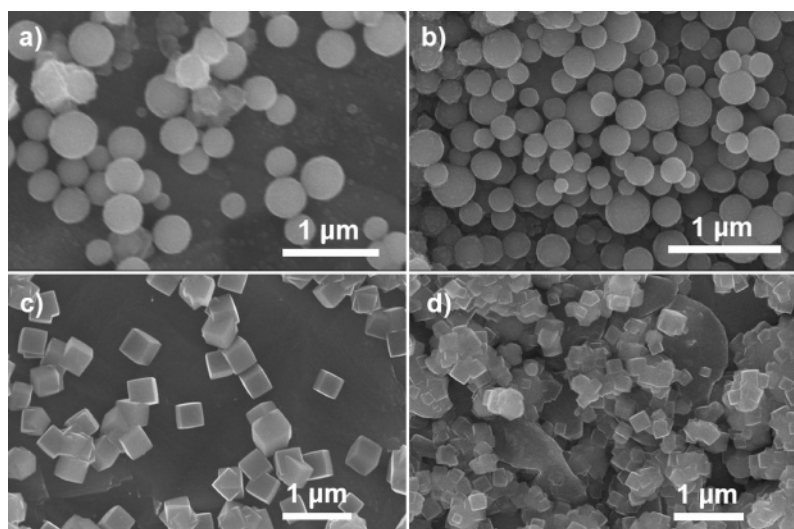


Figure 1. SEM images of Pt nanostructures formed by immersing Cu foils into aqueous solutions of K_2PtCl_4 with different concentrations for 30 min: (a) 0.38 mM; (b) 1.9 mM; (c) 3.8 mM; (d) 38 mM.

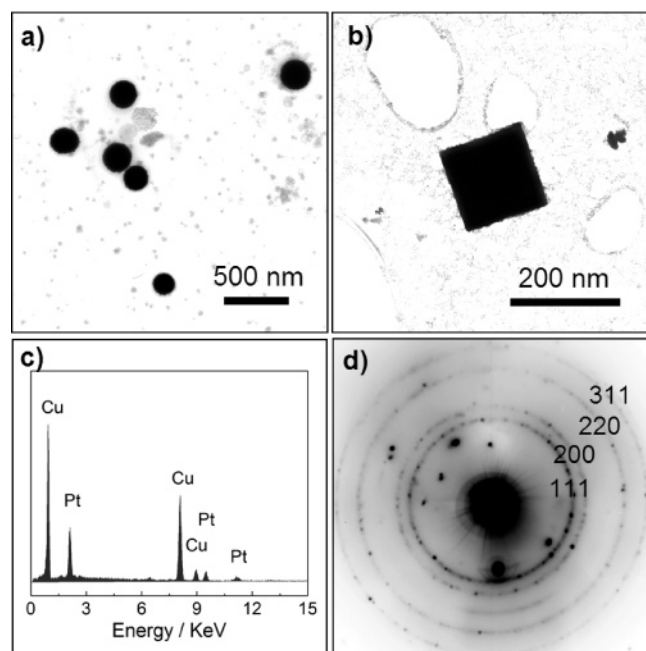
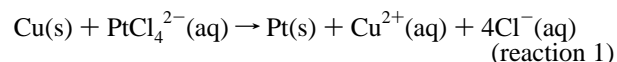


Figure 2. TEM images of (a) spheric and (b) cubic Pt nanoparticles. (c) EDS spectrum and (d) ED pattern of these particles.

to aggregate into clusters (Figure 1d). Similar Au nanospheres and nanocubes have also been produced by immersing the Cu foils into aqueous solutions of HAuCl_4 under similar conditions.

As revealed by the TEM images in Figure 2, parts a and b, the nanospheres and nanocubes are not hollow. The chemical nature of these nanoparticles can be detected by EDS measurements (Figure 2c) to be dominated by Pt signals with several Cu peaks arising from the copper foil substrate. ED patterns for the Pt nanospheres and nanocubes show similar features with several bright concentric rings (Figure 2d), attributable to [111], [200], [220], and [311] crystal planes of a face-centered cubic (fcc) polycrystalline metal Pt (International Centre for Diffraction Data, no. 04-0802).¹⁹

The shape-controlled syntheses of metal nanoparticles have been previously achieved by using capping reagents, such as surfactants and polymers, which selectively bound to certain crystalline face(s) of the growing nanoparticles to retard or enhance the growth from these face(s).^{9a,c,d} Recently, Yang and co-workers^{9e,13a} reported that shape-controlled syntheses of metal nanoparticles could also be realized by introducing foreign metal ions. Elegant work carried out by these authors showed the formation of gold nanocubes through the addition of a small amount of silver ions. By analogy, Cu^{2+} ions produced in the galvanic displacement reaction (i.e., reaction 1) between the Cu foil and K_2PtCl_4 salt solution in our present study could also act as an in situ capping reagent to play the role in regulating the shape of the resulting Pt nanoparticles.



The above scenario was consistent with our observation that the reaction mixture became pale blue, characteristic of Cu^{2+} ions in an aqueous medium, by increasing the K_2PtCl_4 concentration up to 3.8 mM, at which Pt nanocubes were produced (Figure 1c). This observation indicates the importance of Cu^{2+} ions in the formation of Pt nanocubes. The important role of Cu^{2+} ions was further checked by carrying out a control experiment, in which CuCl_2 was deliberately added into an aqueous solution with a low concentration of K_2PtCl_4 (e.g., ≤ 1.9 mM). As expected, the addition of CuCl_2 led to the formation of Pt nanocubes even at the low K_2PtCl_4 concentration (Figure 3, parts a and b), which otherwise should produce Pt nanospheres only (see Figure 1, parts a and b). By prolonging the immersion time of a Cu foil in an aqueous solution of pure K_2PtCl_4 at a low concentration (e.g., ≤ 1.9 mM K_2PtCl_4), we further noticed the formation of hybrid structures with Pt nanocubes growing out from the spheric nanoparticles formed at the low K_2PtCl_4 concentration (Figure 3, parts c and d), indicating a sufficient amount of Cu^{2+} ions have been accumulated during the late stage of the galvanic displacement reaction (i.e., reaction 1). These results provide an effective route toward the formation of hierarchical metal nanostructures—a challenging research topic yet to be explored.

(19) Zoval, J. V.; Lee, J.; Gorer, S.; Penner, R. M. *J. Phys. Chem. B* **1998**, *102*, 1166.

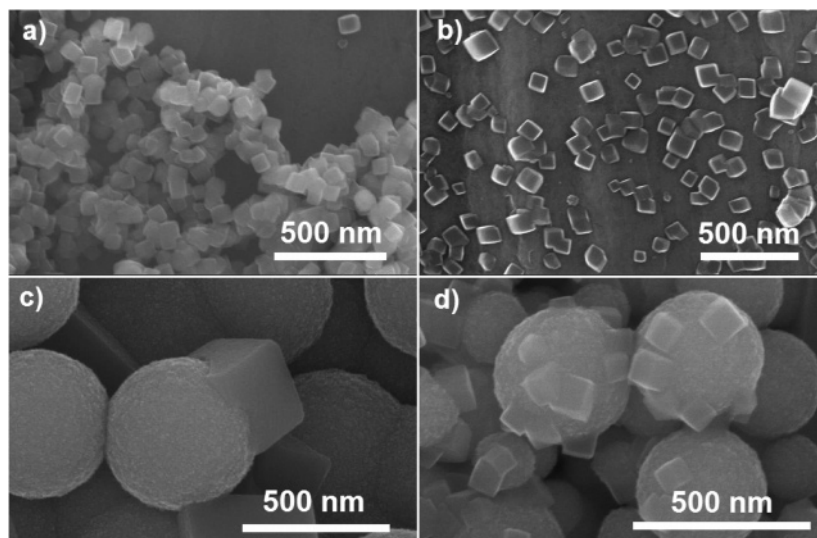


Figure 3. SEM images of Pt nanostructures formed on Cu foils immersed in aqueous solutions of (a) 0.38 mM K_2PtCl_4 and 15 mM $CuCl_2$ for 30 min, (b) 1.9 mM K_2PtCl_4 and 11 mM $CuCl_2$ for 5 min, (c) 1.9 mM K_2PtCl_4 for 80 min, and (d) 0.38 mM K_2PtCl_4 for 140 min.

1.2. Size-Controlled Syntheses of Metal Nanoparticles. As can be seen in Figure 4, there is a strong time dependence of the particle size for the Pt nanoparticles formed via the galvanic displacement reaction (i.e., reaction 1). Upon immersion of the Cu foil into an aqueous solution of K_2PtCl_4 (3.8 mM), cubes of ~ 60 nm in size (i.e., the side length) formed on the copper surface within about 30 s (Figure 4a). After about 2 min, the cubic size increased from ~ 60 nm to ~ 110 nm (Figure 4b). Further increasing the reaction time up to 17 h caused a gradual increase in the cubic size to ~ 700 nm (Figure 4c–i). Also included in Figure 4j is a plot of the cubic size as a function of the reaction time, which clearly indicates a rapid increase in the cubic size at the initial stage of the reaction (less than ca. 30 min), followed by a relatively slow growth of the nanoparticles.

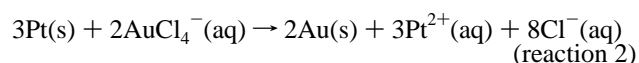
Similar growth kinetics was also observed for the formation of Pt nanospheres on a Cu foil in aqueous solutions of low K_2PtCl_4 concentrations (e.g., ≤ 1.9 mM) at an early stage of the reaction before the appearance of the sphere–cube hybrid structure (cf., Figure 3, parts c and d).

2. Site-Selective Modification of CNTs with the Shape/Size-Controlled Metal Nanoparticles. 2.1. Modification of the Nanotube Outerwall with Metal Nanospheres and Nanocubes. As we can see from the above discussion, the shape- and size-controlled synthetic approaches developed in this study are rather versatile and effective for preparing various metal nanostructures from metal ions of a higher redox potential than that of the Cu foil. This, in conjunction with our previously reported SEED technique,¹⁴ enabled us to site-selectively modify CNTs with metal nanoparticles of a controlled shape and size, as described below.

Figure 5 shows SEM and TEM images for CNTs modified with Pt nanospheres and/or nanocubes along their outerwall by the SEED technique. The Pt nanocube-modified CNTs were prepared by exposing the Cu foil-supported CNTs to an aqueous solution of 3.8 mM K_2PtCl_4 containing 5 mM $CuCl_2$ for 1 min. For the formation of Pt spheric nanoparticles on CNTs, however, the Cu foil-supported CNTs were reacted with an aqueous solution of 0.95 mM K_2PtCl_4 without the addition of $CuCl_2$. Figure 5, parts a and b, shows multisite modification of the

nanotube outerwall in both cases. The corresponding SEM (Figure 5, parts c and d) and TEM (Figure 5, parts e and f) images under higher magnifications clearly show a class of “necklace-like” hybrid structures with individual nanotubes even threading through the nanoparticles. Figure 5g reproduces a typical EDS spectrum for the Pt nanoparticle-modified CNTs supported by a Cu foil, which, as expected, shows a series of Cu, C, and Pt peaks, attributable to the Cu foil substrate, CNTs, and Pt nanoparticles, respectively.

In view of the previous work on gold nanobox formation by a galvanic displacement reaction,^{9a} we further used the nanotube-supported metal nanoparticles prepared above as sacrificial templates for the formation of hollow nanoboxes with a well-defined shape and size (see the Experimental Section). As can be seen in Figure 6, Pt nanocubes (Figure 6, parts a and b; see also Figure 5, parts a and c) can be effectively converted into gold hollow nanoboxes (Figure 6c–f) by depositing Au (nanoparticles) onto the Pt nanocubic faces and dissolving Pt via the following galvanic displacement reaction (i.e., reaction 2).



As expected, the newly formed hollow nanoboxes having side lengths between 200 and 400 nm (Figure 6c–f) are slightly larger than their corresponding nanocube templates (Figure 6, parts a and b) with a fairly rough surface composed of small Au nanoparticles (Figure 6, parts c and d). To image the inside structure of these nanoboxes, we have deliberately removed some cubic face(s) of the nanoboxes by prolonged ultrasonication. As can be clearly seen in Figure 6e, the broken nanoboxes have a hollow chamber with an individual nanotube threading through their cavities. TEM images, as the one shown in Figure 6f, also revealed a hollow structure for these nanoboxes (cf., Figure 2b). The EDS spectrum given in Figure 6g further confirmed the chemical nature of these Au nanoboxes with no detectable Pt. The observed C and Cu peaks are attributable to CNTs and the copper foil substrate, respectively.

Using aligned CNTs as the starting materials, we found that the SEED technique could even be used to deposit metal

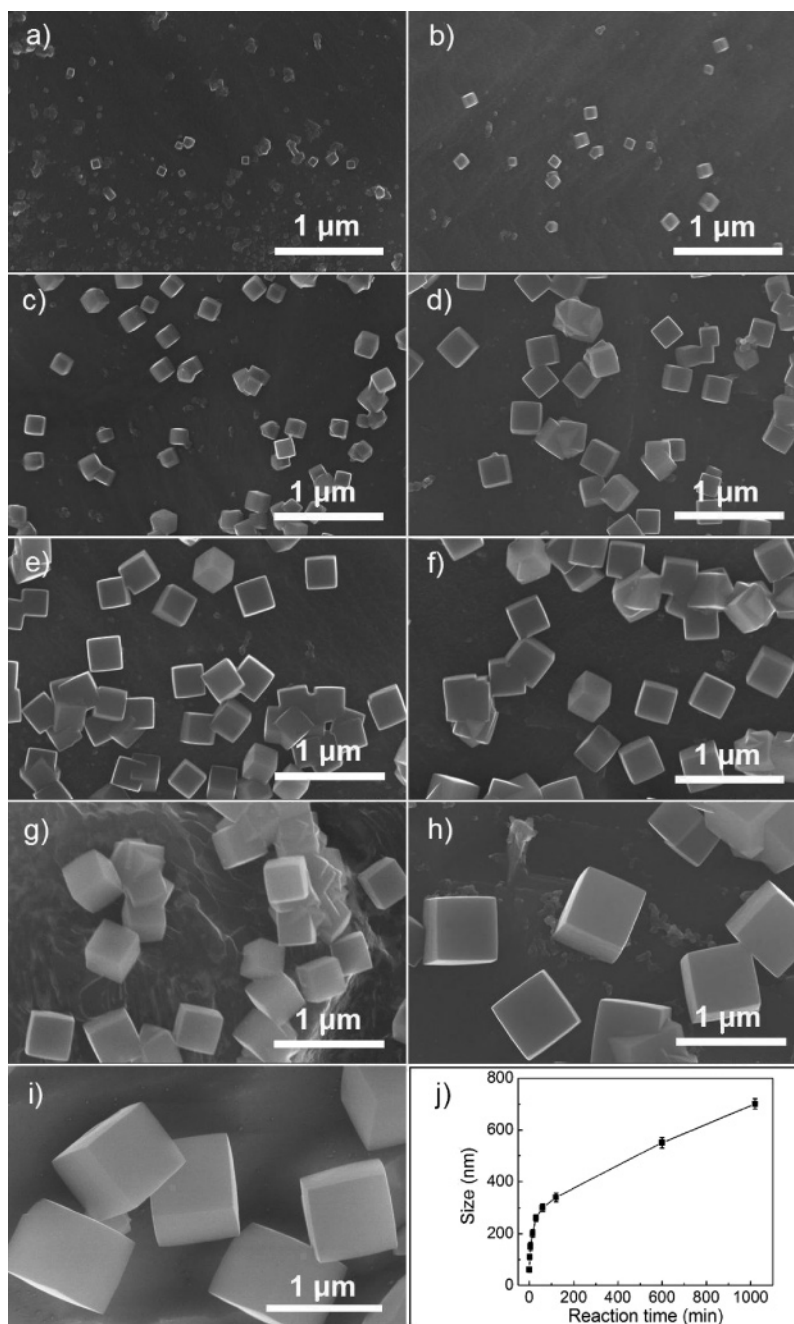


Figure 4. SEM images of Pt nanocubes formed on Cu foils in an aqueous solution of K_2PtCl_4 (3.8 mM) at different reaction times: (a) 30 s; (b) 2 min; (c) 5 min; (d) 15 min; (e) 30 min; (f) 60 min; (g) 2 h; (h) 10 h; (i) 17 h. (j) A typical plot of the cube size vs the reaction time.

nanoparticles along the aligned nanotube structure. As shown in Figure 7a, for instance, Pt nanocubes have been attached onto the aligned CNT outerwall while largely retaining their alignment structure (Figure 7b). Owing to unique physicochemical characteristics of the metal nanoparticles and large surface/interface areas of the aligned nanotube supports, the aligned CNTs decorated with Pt nanoparticles thus prepared offer additional advantages for their use as efficient electrodes, for example in fuel cell, electrochemical sensing, and electrocatalytic systems (vide infra).

2.2. Modification of the Nanotube Innerwall and Asymmetric Sidewall Modification with Metal Nanospheres and Nanocubes. In our previous publication¹⁴ we have briefly mentioned that the inner walls of the template-synthesized

aligned CNTs can also be modified with metal nanoparticles by the SEED technique. In conjunction with the shape-controlled syntheses of metal nanospheres and nanocubes, we have successfully demonstrated in this study that both the innerwall and outerwall of the template-synthesized aligned CNTs can be *asymmetrically* modified with metal nanoparticles of different shapes. Figure 8 shows SEM and TEM images for both the innerwall-modified CNTs (Figure 8, parts a and b) and the asymmetrically modified CNTs with their innerwall being attached with *nanospheres* and outerwall with *nanocubes* (Figure 8, parts c and d). To demonstrate the asymmetric modification of the nanotube sidewalls, we used the template-synthesis technique to directly deposit aligned CNTs into a commercially available alumina membrane according to the reported proce-

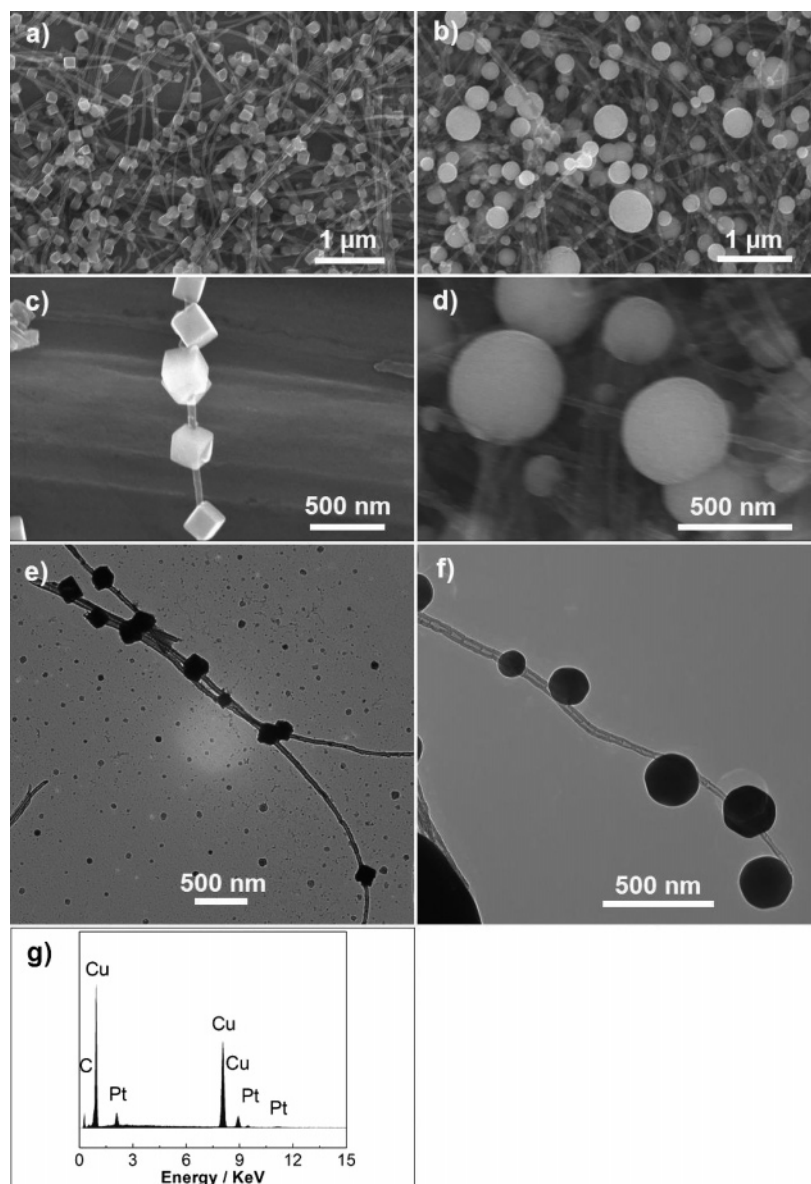


Figure 5. SEM (a–d) and TEM (e and f) images of Pt nanoparticles grafted on the CNTs prepared by immersing Cu-supported CNTs into the aqueous solutions of K_2PtCl_4 under different conditions: (a, c, and e) 3.8 mM K_2PtCl_4 and 5 mM CuCl_2 for 1 min; (b, d, and f) 0.95 mM K_2PtCl_4 for 30 min; (g) a typical EDS spectrum of the Pt nanoparticle–CNT hybrid “necklaces”.

dures.^{13,18} We then carried out the deposition of Pt nanospheres onto the innerwall of the template-synthesized, *perpendicularly* aligned CNTs supported by a Cu foil (Scheme 1b), in which the template acts as a protective layer for the nanotube outerwall. Upon the completion of the innerwall modification, the innerwall-modified nanotubes were released by dissolving the alumina template in aqueous HF. As expected, Figure 8, parts a and b, shows a very smooth outerwall for the innerwall-modified CNTs. The presence of nanospheres within the nanotube innerwall was clearly seen in Figure 8b. To deposit Pt nanocubes onto the outerwall, the innerwall-modified CNTs were supported in a *sidewall-on* configuration (Scheme 1g) on a Cu foil and exposed to an aqueous K_2PtCl_4 solution (3.8 mM) containing 5 mM CuCl_2 for 1 min. While Figure 8c clearly shows the presence of nanocubes on the nanotube outerwall, Figure 8d reveals the asymmetrically modified CNTs with nanocubes and nanospheres deposited onto the nanotube outerwall and innerwall, respectively.

Our TEM examination showed that the outerwall modification did not cause any obvious change of the predeposited Pt nanospheres or any further deposition of Pt nanoparticles on the nanotube innerwall. This is presumably because the *sidewall-on* configuration (Scheme 1g), instead of the *perpendicular* configuration (Scheme 1b) used for the nanotube innerwall modification, of CNTs on the Cu foil allowed electrons required for reducing Pt^{2+} ions to transport from the Cu foil substrate preferentially through the directly touched nanotube outerwalls with a minimized resistance,²⁰ and hence no further Pt deposition on the nanotube innerwall occurred.

2.3. Modification of the Nanotube End-Tips with Metal Nanospheres and Nanocubes. Apart from the nanotube sidewall modification discussed above, we have also demonstrated site-selective deposition of metal nanoparticles on the end-tips of aligned CNTs. Figure 9 shows SEM and TEM images of

(20) Bourlon, B.; Miko, C.; Forro, L.; Glattli, D. C.; Bachtold, A. *Phys. Rev. Lett.* **2004**, *93*, 176806.

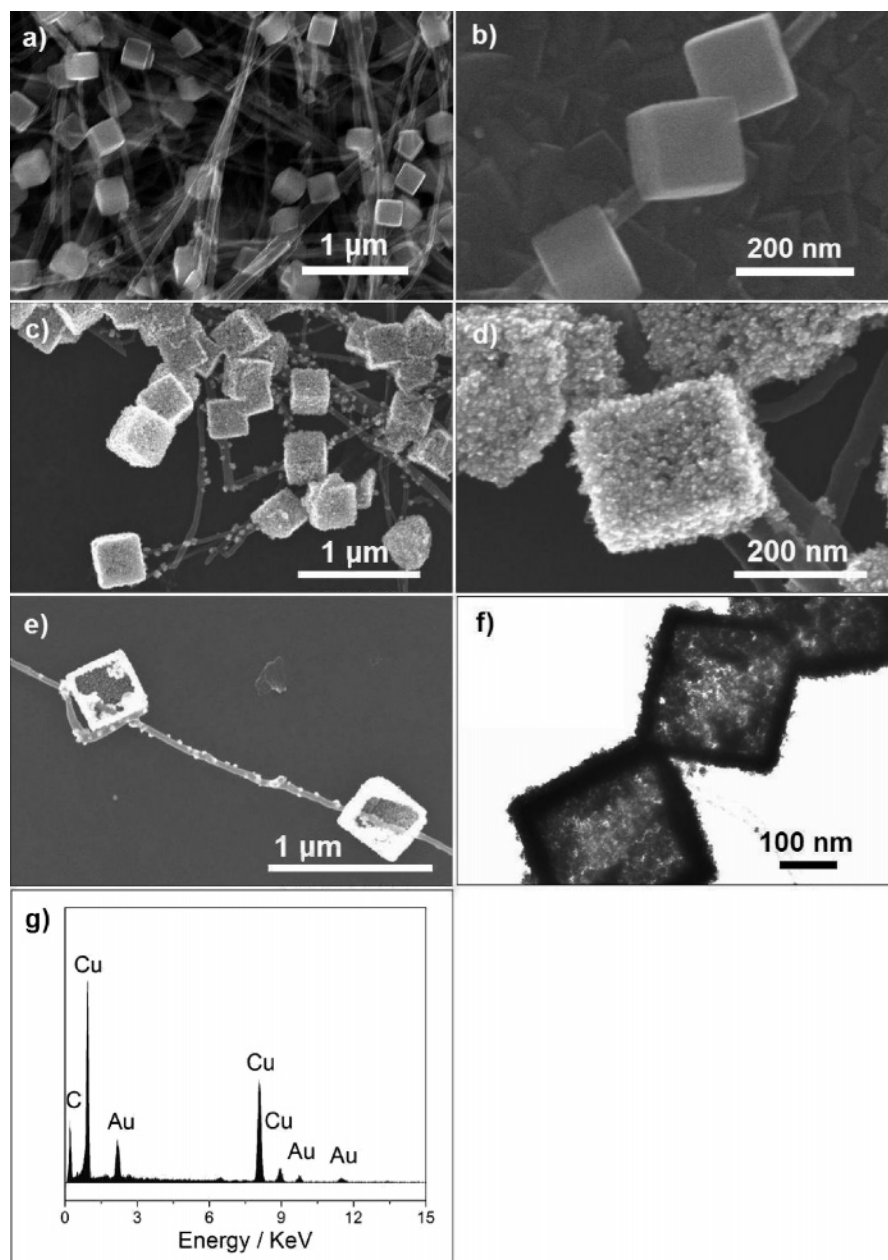


Figure 6. (a and b) SEM images of CNTs grafted with Pt nanocubes at different magnifications prepared by immersing the Cu foil-supported CNTs into an aqueous solution of 3.8 mM K_2PtCl_4 and 5 mM $CuCl_2$ for 1 min. (c–e) SEM images of the nanotube-supported Au nanoboxes generated by exposing the nanotube-supported Pt nanocubes to an aqueous solution of 1 mM $HAuCl_4$ via reaction 2. (f and g) TEM image and EDS pattern of the Au nanobox-decorated CNTs, respectively.

the aligned CNTs with their free end-tips being modified by Pt nanoparticles.

The top-view SEM image given in Figure 9a shows the deposition of Pt nanocubes on the top surface of the aligned CNT film, while the tilt, cross-sectional view SEM image in Figure 9b clearly reveals that these nanocubes were deposited onto the aligned nanotube end-tips with many of the nanotube tips even protruding through the cubes (cf., Figure 5). This peculiar structure was further confirmed by SEM (Figure 9c) and TEM (Figure 9d) images of individual nanotubes dispersed from the tip-modified aligned CNT arrays by ultrasonication. Similar tip-modified nanotube structures were also produced with Pt nanospheres, as exemplified by Figure 9, parts e and f.

3. Optoelectronic Properties of the Nanoparticle-Decorated CNTs. 3.1. Optical Absorption. To study the

optoelectronic properties of the metal nanoparticle-modified CNTs, UV–vis absorption was measured for aqueous solutions (by ultrasonication) of the resultant Pt nanoparticles supported with and without CNTs. Figure 10 shows intensive absorption peaks around 460 nm for the Pt nanocubes and nanospheres. These newly observed optical absorption peaks arise, probably, from the scattering/surface plasmon resonances of the Pt nanoparticles, though further evidence is needed for a more definitive assignment. The appearance of the weak absorption peaks over 270–290 nm are attributable to the presence of some fragmented small Pt nanoparticles²¹ generated through the sonication-induced fragmentation. The corresponding UV–vis absorption spectra for Pt nanocubes and nanospheres attached onto the CNT structure also show similar intensive optical absorption bands as their nanotube-free counterparts but with a

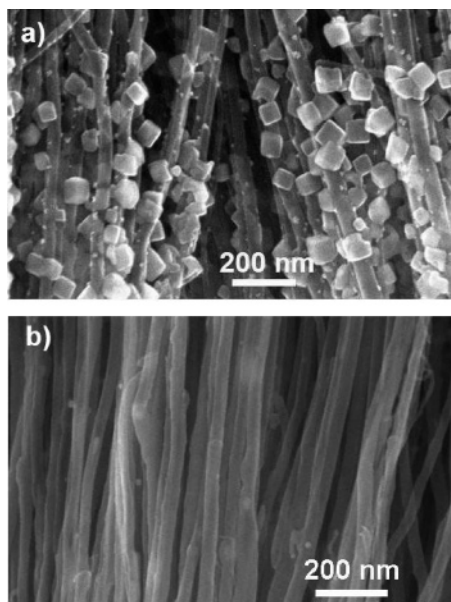


Figure 7. SEM images of (a) aligned CNTs decorated with Pt nanocubes prepared by immersing the Cu foil-supported aligned CNTs into an aqueous solution of 3.8 mM K_2PtCl_4 and 5 mM $CuCl_2$ for 1 min and (b) the pristine aligned CNTs generated by pyrolysis of FePc.

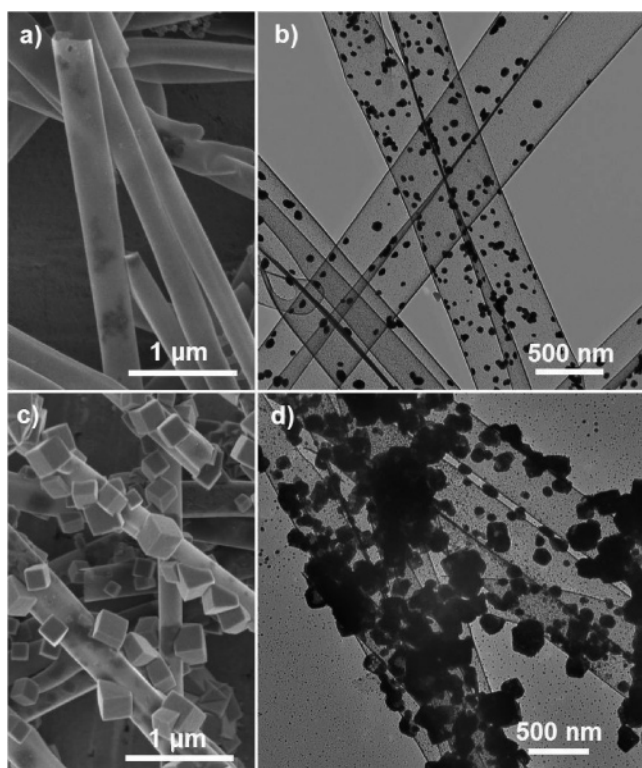


Figure 8. SEM (a) and TEM (b) images of CNTs having their innerwall modified with Pt nanospheres by immersing the template-synthesized, perpendicularly aligned CNTs into an aqueous solution of 1.9 mM K_2PtCl_4 for 30 min. SEM (c) and TEM (d) images of the innerwall-modified CNTs followed by outerwall modification in an aqueous solution of 3.8 mM K_2PtCl_4 containing 5 mM $CuCl_2$ for 1 min with the innerwall-modified CNTs being supported by a Cu foil in a *sidewall-on* configuration (cf. Scheme 1g).

slight red-shift (ca. 50 nm). The red-shift may be attributed to the alignment of metal nanoparticles along the CNT structure.²² No absorption peak was observed above 400 nm for the pristine CNTs, indicating that the intensive absorption peaks seen in

the visible region for the Pt nanoparticle-modified CNTs arise mainly from the nanotube-supported Pt nanoparticles.

3.2. Electrochemical Activities. To study the electrochemical activity of the CNTs modified with metal nanoparticles, we used the FePc-generated aligned CNTs modified with Pt nanocubes as the working electrode (cf., Figure 7a) for electrocatalytic oxidation of methanol. In a control experiment, the pristine aligned CNT electrode (cf., Figure 7b) was measured under the same condition for comparison. As can be seen in Figure 11, the pristine aligned CNT electrode showed a capacitive current only due to the double layer capacitance (Figure 11a), whereas the Pt nanoparticle-grafted aligned CNT electrode showed two strong redox peaks at 0.45 and 0.7 V characteristic of methanol oxidation.²³ These results indicate the usefulness of the metal nanoparticle-modified aligned CNT arrays as efficient electrodes in methanol direct fuel cells and perhaps many other electrochemical systems.

Conclusions

In summary, we have demonstrated a simple and versatile route for shape/size-controlled syntheses of Pt and Au nanoparticles by the galvanic displacement reaction of a Cu foil with K_2PtCl_4 and $HAuCl_4$ in an aqueous medium under different conditions. Both the shape and size of the resultant metal nanoparticles were found to strongly depend on the metal salt concentration and reaction time, providing considerable room for regulating morphologic features of the resultant nanoparticles. Of particular interest, Pt nanospheres, nanocubes, and hybrid nanoparticles with the nanocube(s) growing out from the nanospheres were produced.

In conjunction with our previously reported SEED technique, the shape/size-controlled syntheses have been successfully exploited to deposit the metal nanoparticles onto CNTs in a site-selective fashion. In particular, Pt nanocube(s) or nanosphere(s) have been site-selectively grafted onto the nanotube outerwall, innerwall, or end-tip. Furthermore, we have also demonstrated the asymmetric sidewall modification by attaching the innerwall and outerwall of individual CNTs with metal nanoparticles of different shapes. The nanotube-supported Pt nanoparticles were further converted into Au hollow nanoboxes by galvanic displacement reaction of Pt with Au.

The resultant CNTs modified with metal nanoparticles of different shape and size showed interesting optoelectronic properties. The Pt nanocubes (100–200 nm) and nanospheres (200–500 nm) showed intensive optical absorption bands centered at about 460 nm, while their counterparts supported by CNTs showed similar optical absorption bands with a red-shift (ca. 50 nm) due to the alignment of these metal nanoparticles along the nanotube structure. On the other hand, the Pt nanoparticle-decorated aligned CNT electrodes were demonstrated to be highly electroactive with respect to the correspond-

- (21) (a) Chen, C. W.; Akashi, M. *Langmuir* **1997**, *13*, 6465. (b) Fu, X. Y.; Wang, Y.; Wu, N. Z.; Gui, L. L.; Tang, Y. Q. *Langmuir* **2002**, *18*, 4619. (c) Huang, J. C.; Liu, Z. L.; Liu, X. M.; He, C. B.; Chow, S. Y.; Pan, J. S. *Langmuir* **2005**, *21*, 699. (d) Zhou, M.; Chen, S. H.; Ren, H. P.; Wua, L.; Zhao, S. Y. *Physica E* **2005**, *27*, 341. (e) Henglein, A.; Ershov, B. G.; Malow, M. *J. Phys. Chem.* **1995**, *99*, 14129.
- (22) Correa-Duarte, M. A.; Pérez-Juste, J.; Sánchez-Iglesias, A.; Giersig, M.; Liz-Marzán, L. M. *Angew. Chem. Int. Ed.* **2005**, *44*, 4375.
- (23) (a) Yahikozawa, K.; Fujii, Y.; Mitsuuda, Y.; Nishimura, K.; Takasu, Y. *Electrochim. Acta* **1991**, *36*, 973. (b) Guo, D. J.; Li, H. L. *J. Electroanal. Chem.* **2004**, *573*, 197. (c) Tang, H.; Chen, J. H.; Wang, M. Y.; Nie, L. H.; Kuang, Y. F.; Yao, S. Z. *Appl. Catal., A* **2004**, *275*, 43.

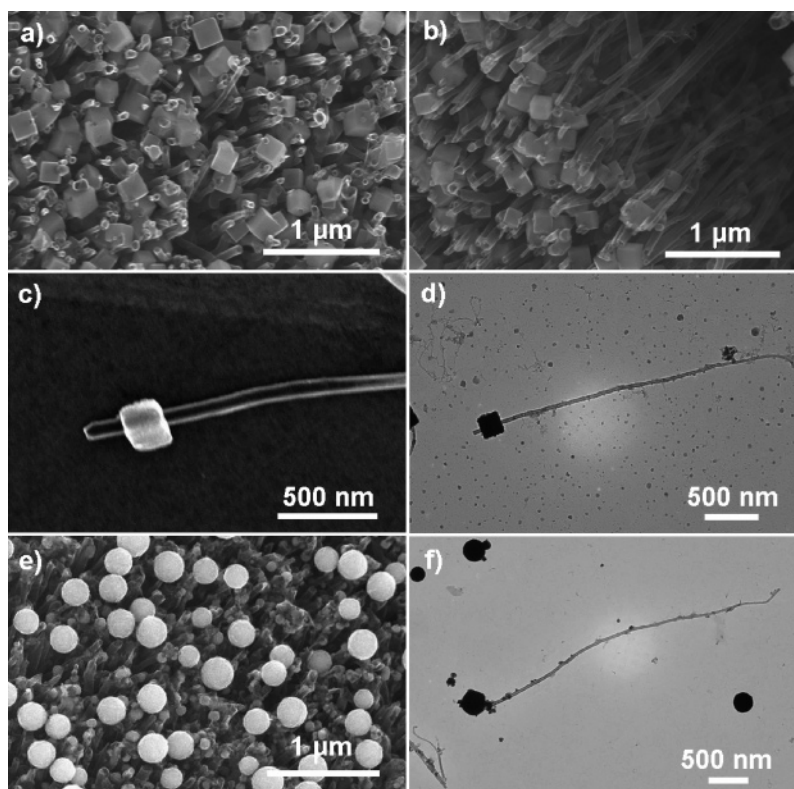


Figure 9. SEM (a–c) and TEM (d) images of Pt nanocubes deposited onto the nanotube tips by floating the Cu foil-supported aligned CNT films on an aqueous solution of 3.8 mM K_2PtCl_4 containing 5 mM $CuCl_2$ for 1 min. SEM (e) and TEM (f) images of Pt nanospheres deposited onto the nanotube tips by floating the Cu foil-supported aligned CNT films on an aqueous solution of 0.95 mM K_2PtCl_4 for 30 min.

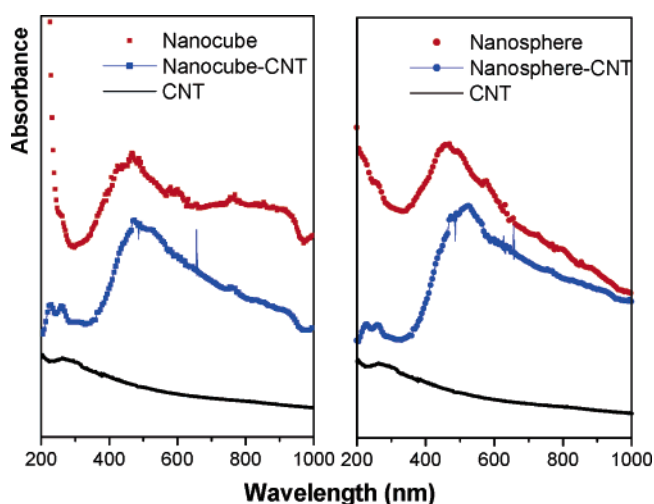


Figure 10. UV-vis spectra of the pristine CNTs, Pt nanocubes (■, ~100–200 nm), Pt nanospheres (●, ~200–500 nm), and the corresponding metal nanoparticle-modified CNTs dispersed in water by ultrasonication.

ing pristine aligned CNT electrodes. Therefore, the newly developed technique for the shape/size-controlled syntheses of metal nanoparticles for the site-selective modification of CNTs are very attractive for producing various multicomponent nanoparticle–nanotube hybrid structures useful in a wide range of potential applications, including fuel cell, catalytic, sensing, and optoelectronic systems.

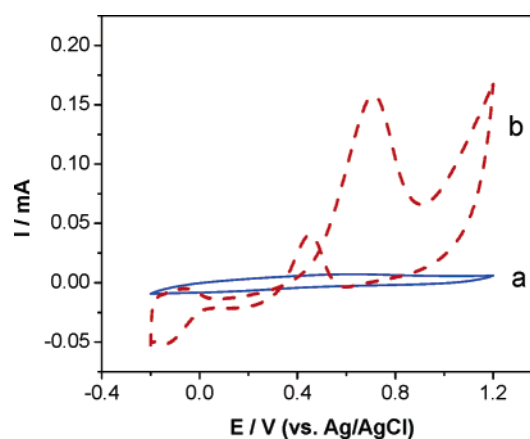


Figure 11. Cyclic voltammograms of (a) the pristine aligned CNT and (b) Pt nanoparticle-modified aligned CNT electrodes supported by a sputter-coated Au layer in a N_2 -saturated aqueous solution of 2 M CH_3OH + 0.1 M H_2SO_4 solution (scan rate, 50 mV/s).

Acknowledgment. We thank NSF (CCF-0403130), NEDO (04IT4), ACS (PRF 39060-AC5M), WCI/CMPND, AFRL/ML, the Wright Brothers Institute, the Dayton Development Collation, and the University of Dayton for financial support. Thanks also to the NEST Lab at UD for the access of the SEM and TEM facilities. We are grateful to Dr. Dave Anderson and Dr. Tia Benson Tolle for their kind help and strong support.

JA060296U